The hidden role of multi-trophic interactions in driving diversity-productivity relationships

Georg Albert[1,2], Benoit Gauzens[1,2], Michel Loreau[3], Shaopeng Wang[4], Ulrich Brose[1,2]

1 EcoNetLab, German Centre for Integrative Biodiversity Research (iDiv) Halle-Jena-Leipzig, 04103 Leipzig, Germany.

2 Institute of Biodiversity, Friedrich Schiller University Jena, 07743 Jena, Germany.

3 Theoretical and Experimental Ecology Station, CNRS and Paul Sabatier University, 09200 Moulis, France.

4 Institute of Ecology, College of Urban and Environmental Sciences, and Key Laboratory for Earth Surface Processes of the Ministry of Education, Peking University, 100871 Beijing, China.

This supplementary document includes:

Supplementary 1: Detailed description of simulation model

Supplementary Figures S1-12

Supplementary 1: Detailed description of simulation model

We used an allometric-trophic-network model to simulate the complex trophic dynamics of ecosystems in a controlled environment (Schneider et al. 2016). It defines trophic interactions between different species based on their body-mass ratios and utilizes a set of differential equations that describes density changes of resources, producers, and animal consumers over time.

Simulating producer-resource interactions

The change in biomass density P_i of primary producer species i is calculated as

$$\frac{dP_i}{dt} = r_i G_i P_i - \sum_k A_k F_{ki} - x_i P_i,$$

with the first term describing resource-dependent growth, the second describing mortality due to predation by animals, and the third describing metabolic demands. Both the intrinsic growth rate r_i of species i, which defines its maximum possible growth rate, and the metabolic demands x_i of species i scale allometrically with body mass (Enquist et al. 1998; Stephenson et al. 2014):

$$r_i = m_i^{-0.25},$$

$$x_i = x_P m_i^{-0.25}.$$

with $m_i = 10^{\mu_P}$ being the specific body mass of producer species i, where μ_P follows a uniform distribution on [0, 6]. Metabolic demands were rescaled by x_P = 0.138 (Brose 2008). Growth of primary producer species i was further limited by the species specific growth factor G_i, defined by two limiting resource j ϵ {1, 2} as

$$G_i = min\left(\frac{\theta_{i1}}{K_{i1}+\theta_{i1}}, \frac{\theta_{i2}}{K_{i2}+\theta_{i2}}\right),$$

where K_{ij} is the half-saturation density of resource j at which the resource uptake rate of primary producer i is half of its maximum, and follows a uniform distribution on [0.1, 0.2]. θ_{ij} is the concentration of resource j accessible by primary producer i.

To simulate different scenarios of resource-use dissimilarity (RUD; see methods in main text), we spread resource concentrations of each considered resource j across C = 16 resource compartments. The change in resource concentrations N_{jn} of resource j in resource compartment n was defined as:

$$\frac{dN_{jn}}{dt} = D\left(\frac{S_j}{C} - N_{jn}\right) - v_j \sum_i r_i G_i P_i \frac{N_{jn}}{\theta_{ij}}.$$

The first term describes the rate at which resources are renewed. It is limited by the turnover rate D, which was set to 0.25. The supply concentration S_j represents the maximum concentration of resource j. It was set to 50 and 25 for resources 1 and 2, respectively. As we defined each compartment n to be quantitatively the same, we split the supply concentration S_j equally between compartments. The second term captures the loss of resources due to primary production, which is similar to the resource-dependent growth term used to calculate the change in primary producer densities but separated for each resource compartment. The relative content of resource j in the biomass of primary producers is described as v_j and was set to 1 and 0.5 for resources 1 and 2, respectively. By keeping the ratio between S_j and v_j the same for both resources j, all resources considered can limit the growth of primary producers and consequently play a role in determining competitive advantages while contributing differently to primary production. The pool of resource j accessible by producer species i corresponds to the sum of resource concentrations in the compartments it has access to:

$$\theta_{ij} = \sum_n \vartheta_{¿} N_{jn},$$

with $\vartheta_{¿} = 1$ if species i can access resource compartment n, $\vartheta_{¿} = 0$ otherwise.

At the end of the simulations, we quantified primary production as the summed up resource uptake of both resources j, in all compartments n, and for all primary producer species i:

$$Y = \sum_i Y_i = \sum_j \sum_n v_j \sum_i r_i G_i P_i \frac{N_{jn}}{\theta_{ij}}.$$

Creating network topology and simulating animal consumers

Similar to primary producer species, each animal species k was characterized by its specific body mass $m_k = 10^{\mu_A}$ with the exponents drawn randomly from a uniform distribution on [2, 12]. To create a viable network topology, we calculated the probability of consumer species x to feed on an encountered resource species z as

$$L_{xz} = \left(\frac{m_x}{m_z R_{opt}} e^{1 - \frac{m_x}{m_z R_{opt}}} \right)^{\gamma},$$

with the optimal consumer-resource body mass ratio R_{opt} = 100 and γ = 2. Low probabilities with $L_{xz} \leq 0.01$ were set to be zero. We only considered animal communities where each species had at least one resource species at maximum producer richness (i.e., 16 producer species). When lowering producer richness (see main text), animal species that lost their resource species were removed before simulations.

The change of biomass densities of species k, A_k over time, was simulated as

$$\frac{d A_k}{dt} = e_P A_k \sum_i F_{ki} + e_A A_k \sum_l F_{kl} - \sum_l A_l F_{lk} - x_k A_k,$$

with the first term describing increases due to the summed up herbivorous feeding on primary producer species i, with a conversion efficiency e_P = 0.545 (Lang et al. 2017). Similarly, the second term describes the summed up carnivorous feeding on animal species i, with a conversion efficiency of e_A = 0.906 (Lang et al. 2017). The third term captures mortality due to predation by animals i in the

same way as for primary producers. The last term represents metabolic demands of animal species k, which scales allometrically with body mass (Ehnes et al. 2011) as

$$x_k = x_A m_k^{-0.305},$$

with a scaling constant x_A = 0.141 (Ehnes et al. 2011). All trophic interactions include feeding rates

$$F_{xz} = \frac{\omega_x b_{xz} Z_z^{1+q_{xz}}}{1 + c X_x + \omega_x \sum_\zeta b_{x\zeta} h_{x\zeta} Z_\zeta^{1+q_{x\zeta}}} \cdot \frac{1}{m_x}$$

as a function of the biomass densities X_x and Z_z of the consumer species x and resource species z, respectively. Feeding rates capture the proportion of biomass of resource species z consumer species x consumes. By dividing by body mass, the per-capita feeding rate is transformed to be relative to one unit biomass. Consumers with multiple resource species have to split their feeding efforts, captured in the relative consumption rate ω_x, defined as the inverse of the number of prey species of consumer x. Time lost due to consumer interference c was drawn from a normal distribution (μ_c = 0.8, σ_c = 0.2) for each food web. We used an interaction-specific, allometric Hill-exponent $1 + q_{xz}$ (Kalinkat et al. 2013), which determines the functional response type of the interaction. It was calculated as:

$$q_{xz} = \frac{q_{max} R_{xz}^2}{q_0^2 + R_{xz}^2},$$

with R_{xz} being the consumer-resource body mass ratio of consumer species x and resource species z. By setting q_{max} = 1, we assure that the functional response varies between the classic type II (q_{xz} = 0) and type III (q_{xz} = 1). At optimal consumer-resource body mass ratio R_{opt} = 100 we wanted q_{xz} to be at intermediate levels. Therefore, we also set q_0 = 100. At higher consumer-resource body mass ratios, the functional response gets closer to the classic type III, which lowers the feeding rates at low resource densities. The feeding rate was further determined by the capture coefficient:

$$b_{xz} = b_0 m_x^{\beta_x} m_z^{\beta_z} L_{xz},$$

which describes the success rate of consumer species x to capture resource species z. It is based on the assumption that an encounter is more likely with higher movement speeds of both consumer and resource species. Since movement speed scales allometrically and based on feeding type (Hirt et al. 2017), we drew β_x and β_z from according normal distributions (carnivore: $\mu_\beta = 0.42$, $\sigma_\beta = 0.05$, omnivore: $\mu_\beta = 0.19$, $\sigma_\beta = 0.04$, herbivore: $\mu_\beta = 0.19$, $\sigma_\beta = 0.04$, primary producer: $\mu_\beta = 0$, $\sigma_\beta = 0$). Similarly, we assumed different values for b_0 based on the feeding type of the consumer (carnivore: $b_0 = 50$, omnivore: $b_0 = 100$, herbivore: $b_0 = 200$). The handling time:

$$h_{xz} = h_0 m_x^{\eta_x} m_z^{\eta_z},$$

scales with the body mass of consumer and resource species to the power of η_x ($\mu_{\eta_x} = -0.48$, $\sigma_{\eta_x} = 0.03$) and η_z ($\mu_{\eta_z} = -0.66$, $\sigma_{\eta_z} = 0.02$) respectively. The scaling constant h_0 was set to 0.4. All parameters drawn from normal distributions had to fall within the inclusive limits of $\mu \pm 3\sigma$ or be redrawn otherwise.

Simulation setup

Initial biomass densities of primary producer and animal species were randomly drawn from uniform distributions on [0, 1]. Resource densities were initialized for the whole resource pool with random values drawn from uniform distributions on $[S_j / 2, S_j]$, which were then evenly split between compartments. We ran simulations until $t = 150.000$. Species that reached biomass densities < 10^{-6} during simulations were assumed to be extinct, and their values were set to 0.

We ran all simulations in Julia 1.2.0 (Bezanson et al. 2017) using the DifferentialEquations package (Rackauckas & Nie 2017) and utilizing a stiffness detection algorithm that automatically switched between the solvers Vern7 for non-stiff problems and Rodas4 for stiff problems.

References

Bezanson, J., Edelman, A., Karpinski, S. & Shah, V.B. (2017). Julia: A fresh approach to numerical computing. *SIAM Rev.*, 59, 65–98.

Brose, U. (2008). Complex food webs prevent competitive exclusion among producer species. *Proc. R. Soc. B Biol. Sci.*, 275, 2507–2514.

Ehnes, R.B., Rall, B.C. & Brose, U. (2011). Phylogenetic grouping, curvature and metabolic scaling in terrestrial invertebrates. *Ecol. Lett.*, 14, 993–1000.

Enquist, B.J., Brown, J.H. & West, G.B. (1998). Allometric scaling of plant energetics and population density. *Nature*, 395, 163–165.

Hirt, M.R., Lauermann, T., Brose, U., Noldus, L.P.J.J. & Dell, A.I. (2017). The little things that run: a general scaling of invertebrate exploratory speed with body mass. *Ecology*, 98, 2751–2757.

Kalinkat, G., Schneider, F.D., Digel, C., Guill, C., Rall, B.C. & Brose, U. (2013). Body masses, functional responses and predator-prey stability. *Ecol. Lett.*, 16, 1126–1134.

Lang, B., Ehnes, R.B., Brose, U. & Rall, B.C. (2017). Temperature and consumer type dependencies of energy flows in natural communities. *Oikos*, 126, 1717–1725.

Rackauckas, C. & Nie, Q. (2017). DifferentialEquations.jl – A Performant and Feature-Rich Ecosystem for Solving Differential Equations in Julia. *J. Open Res. Softw.*, 5.

Schneider, F.D., Brose, U., Rall, B.C. & Guill, C. (2016). Animal diversity and ecosystem functioning in dynamic food webs. *Nat. Commun.*, 7, 1–8.

Stephenson, N.L., Das, A.J., Condit, R., Russo, S.E., Baker, P.J., Beckman, N.G., *et al.* (2014). Rate of tree carbon accumulation increases continuously with tree size. *Nature*, 507, 90–93.

Figure S1: Effects of resource-use dissimilarity on net diversity effects ΔY of the primary producer community. Effects are shown for different levels of producer (rows) and multi-trophic animal richness (columns). Error bars show 25th and 75th; squares show 50th percentile (i.e., median).

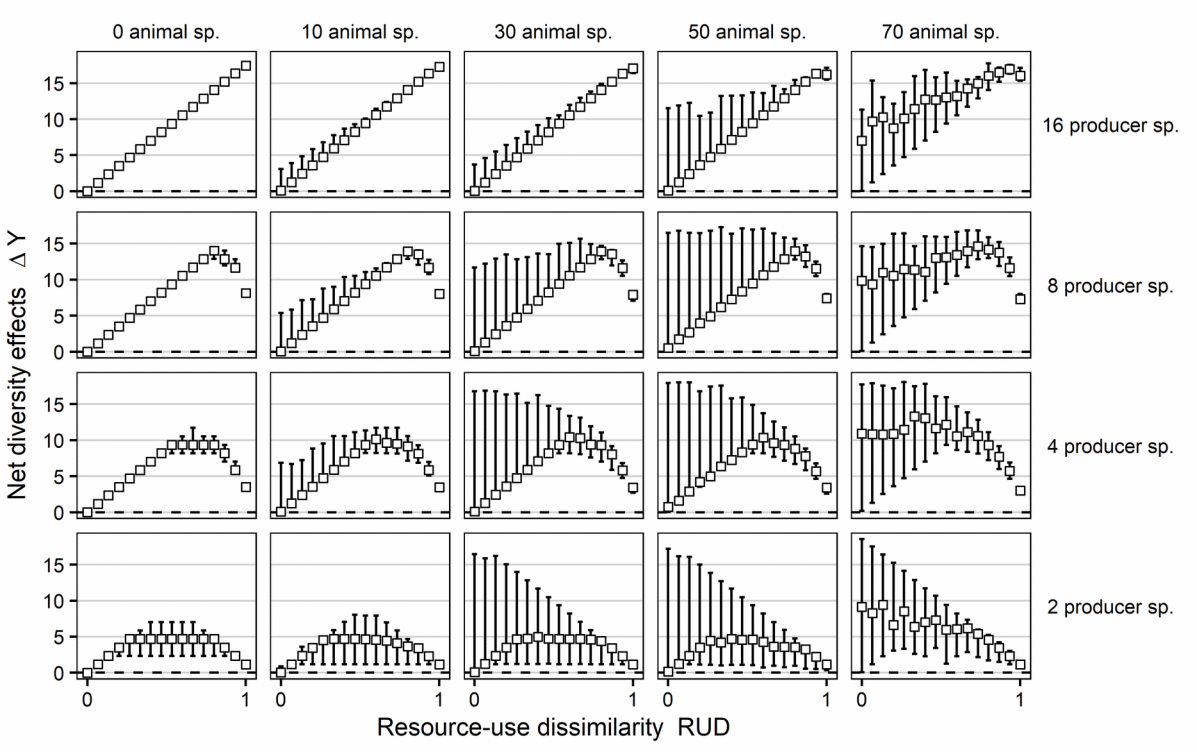

146 **Figure S2:** Effects of resource-use dissimilarity RUD on complementarity effects CE of primary
147 productivity. Effects are shown for different levels of producer (rows) and multi-trophic animal
148 richness (columns). Error bars show 25th and 75th; squares show 50th percentile (i.e., median).

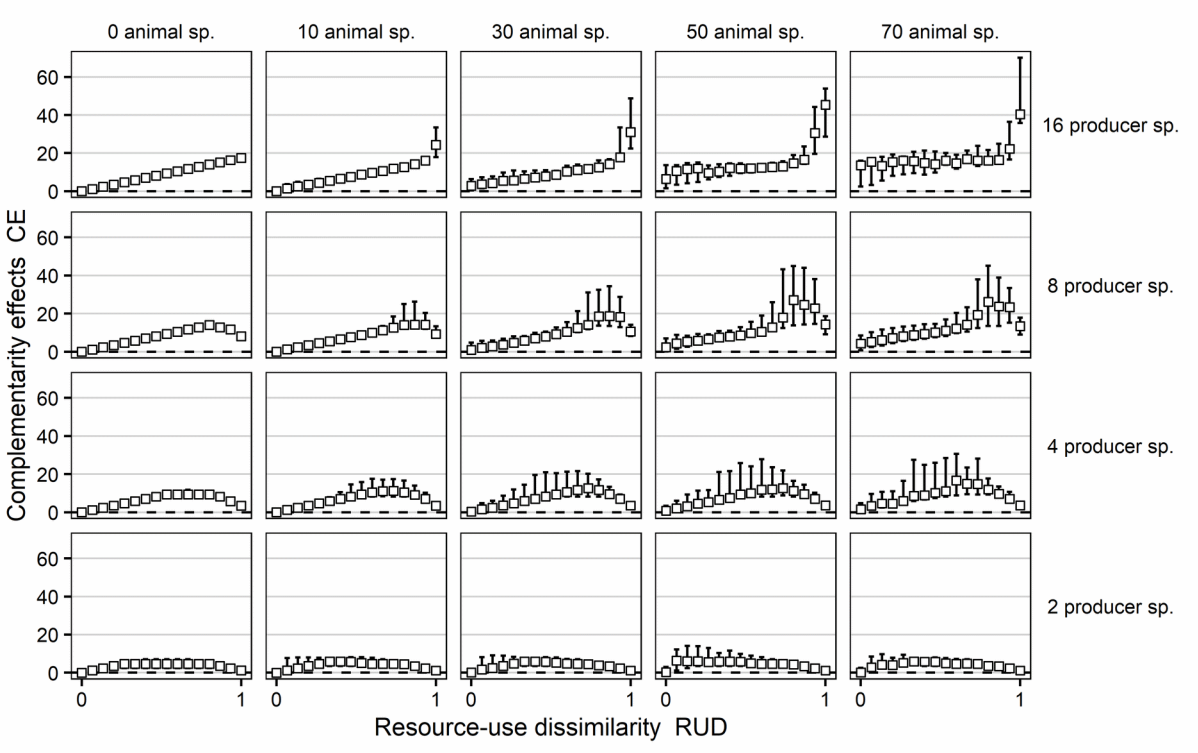

149

Figure S3: Effects of resource-use dissimilarity RUD on selection effects SE of primary productivity. Effects are shown for different levels of producer (rows) and multi-trophic animal richness (columns). Error bars show 25th and 75th; squares show 50th percentile (i.e., median).

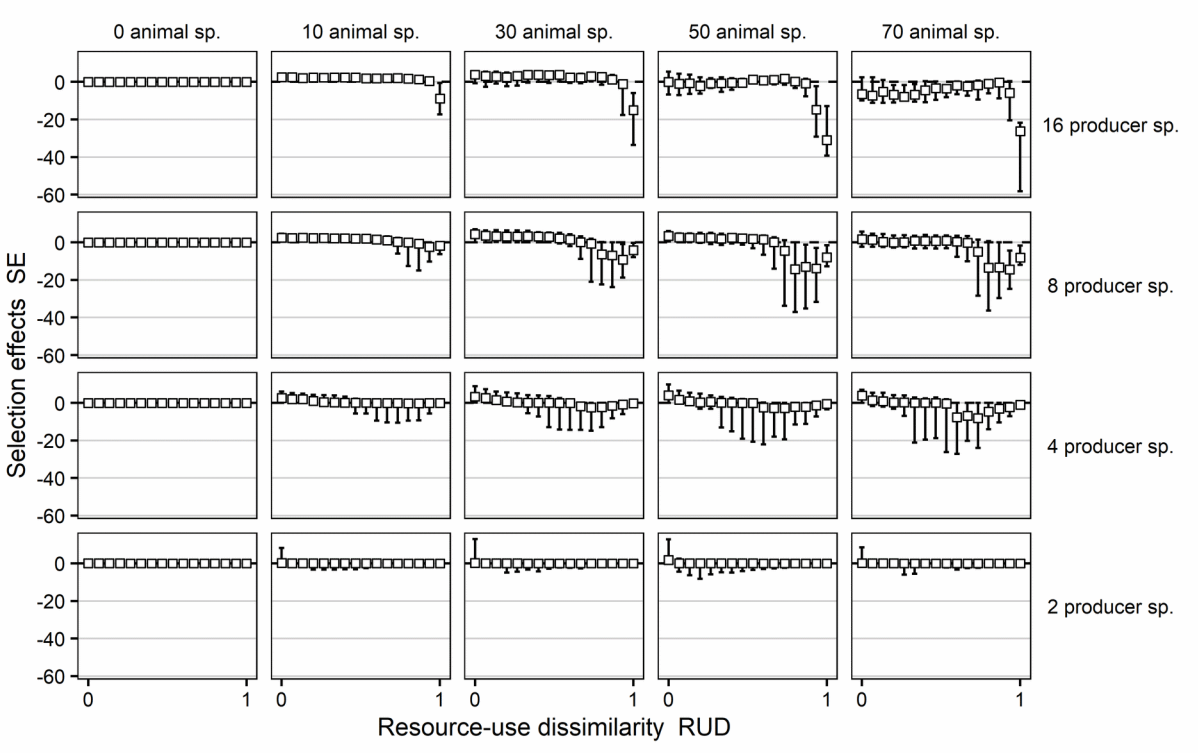

Figure S4: Effects of resource-use dissimilarity RUD on the Shannon diversity of primary producers' resource-use H_{exp}. Effects are shown for different levels of producer (rows) and multi-trophic animal richness (columns). Error bars show 25th and 75th; squares show 50th percentile (i.e., median).

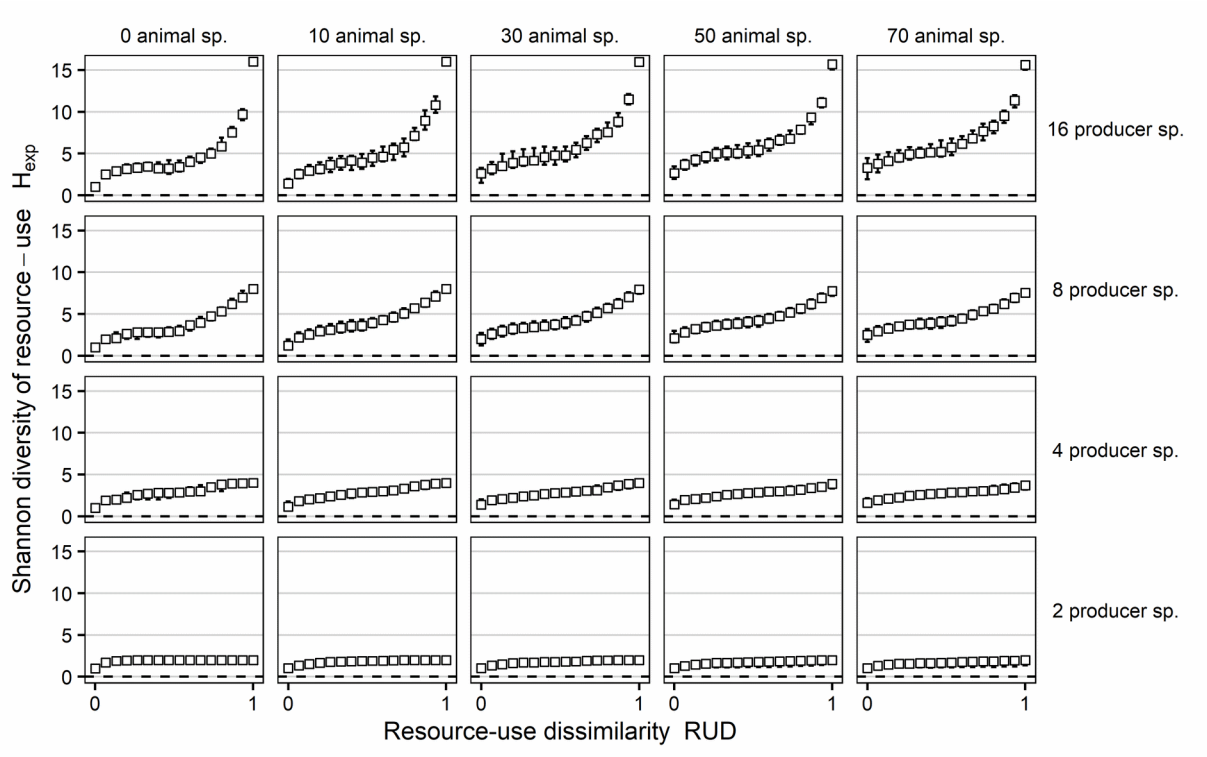

Figure S5: Effects of resource-use dissimilarity RUD on the relative survival of the primary producer community. Effects are shown for different levels of producer (rows) and multi-trophic animal richness (columns). Error bars show 25th and 75th; squares show 50th percentile (i.e., median).

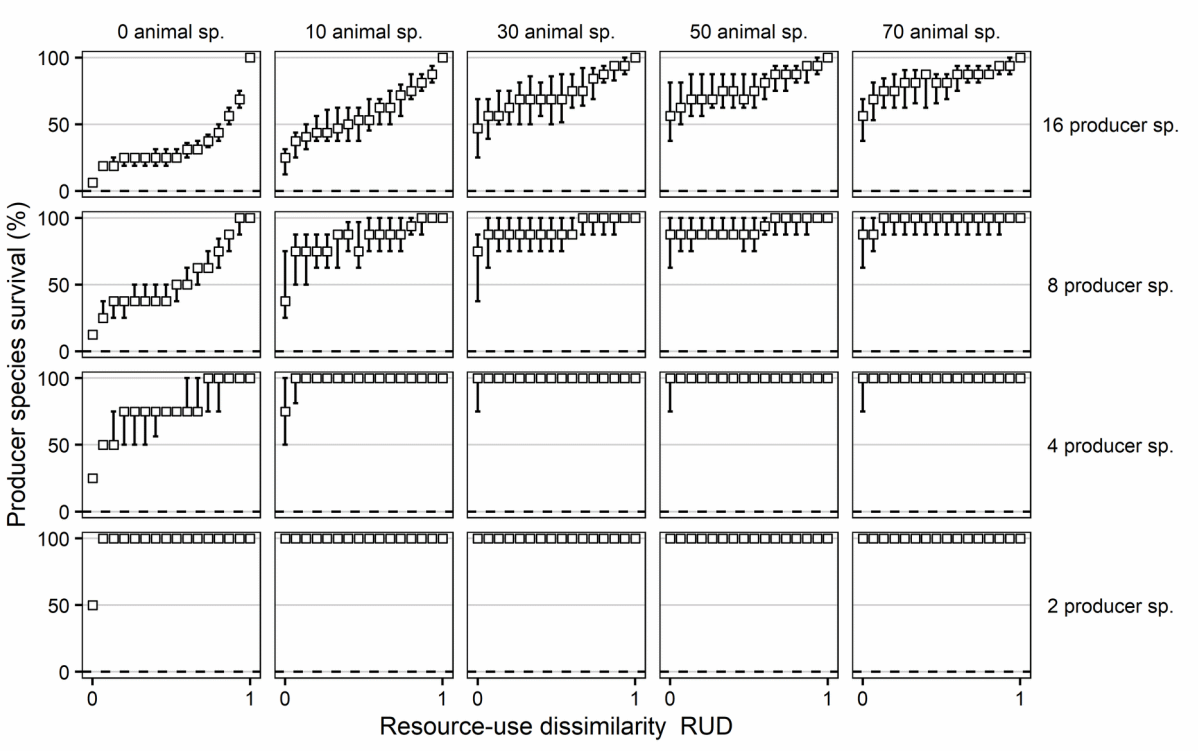

Figure S6: Effects of resource-use dissimilarity RUD on observed yield Y_O (blue) and expected yield Y_E (red) of the primary producer community. Effects are shown for different levels of producer (rows) and multi-trophic animal richness (columns). Error bars show 25th and 75th; squares show 50th percentile (i.e., median).

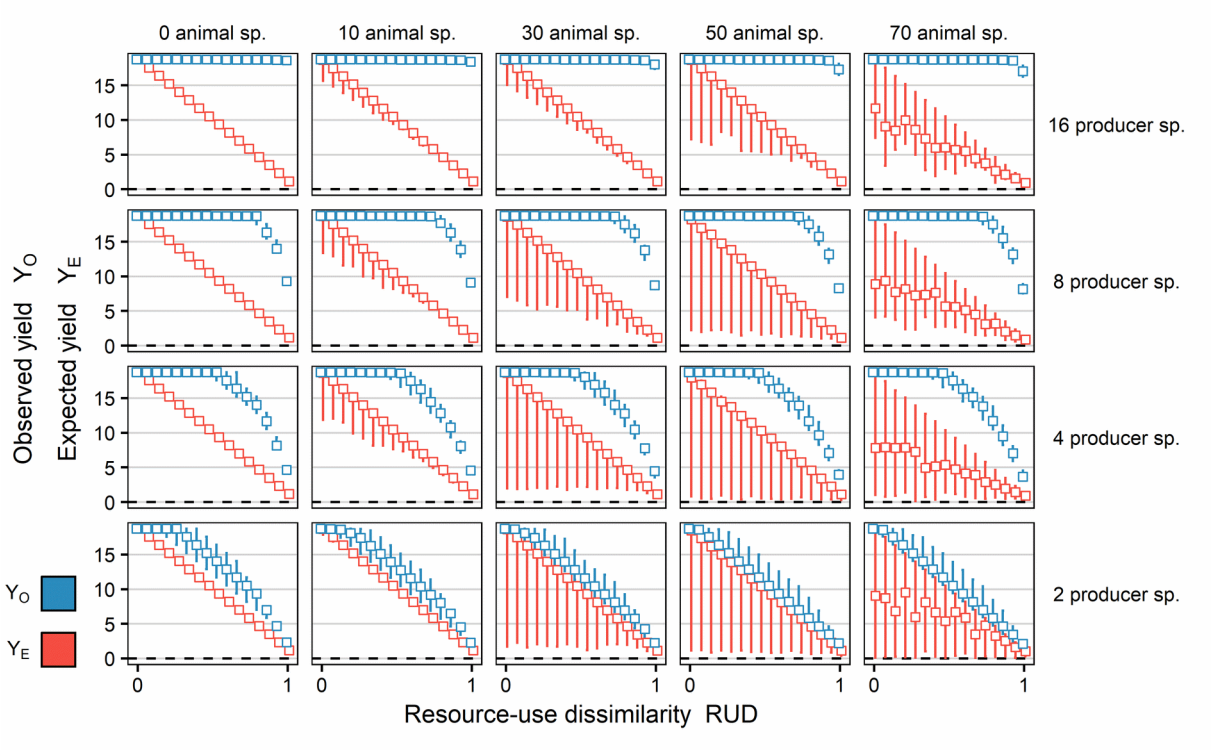

Figure S7: Effects of relative primary producer species survival on complementarity effects CE. Effects are shown for different levels of producer (rows) and multi-trophic animal richness (columns). The level of resource-use dissimilarity (RUD) is indicated by the color (yellow: low, purple: high). To improve readability, only 95% of the simulated food webs are shown.

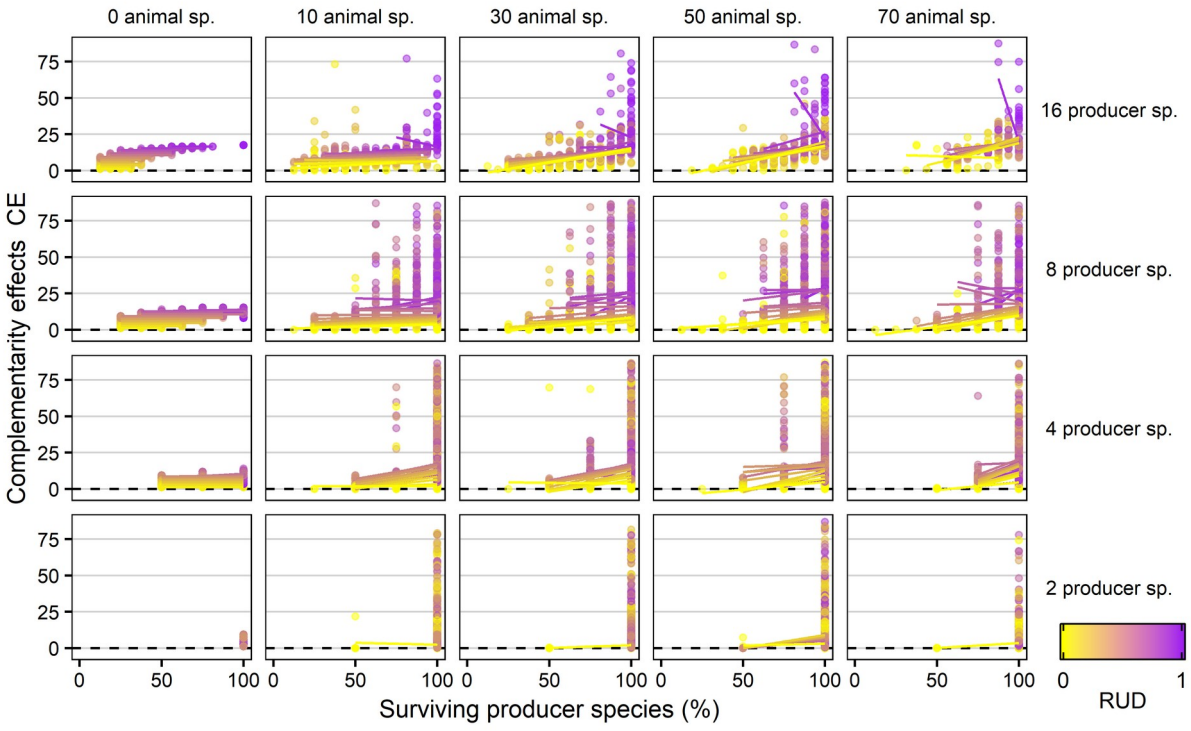

Figure S8: Effects of relative primary producer species survival on selection effects SE. Effects are shown for different levels of producer (rows) and multi-trophic animal richness (columns). The level of resource-use dissimilarity (RUD) is indicated by the color (yellow: low, purple: high). To improve readability, only 95% of the simulated food webs are shown.

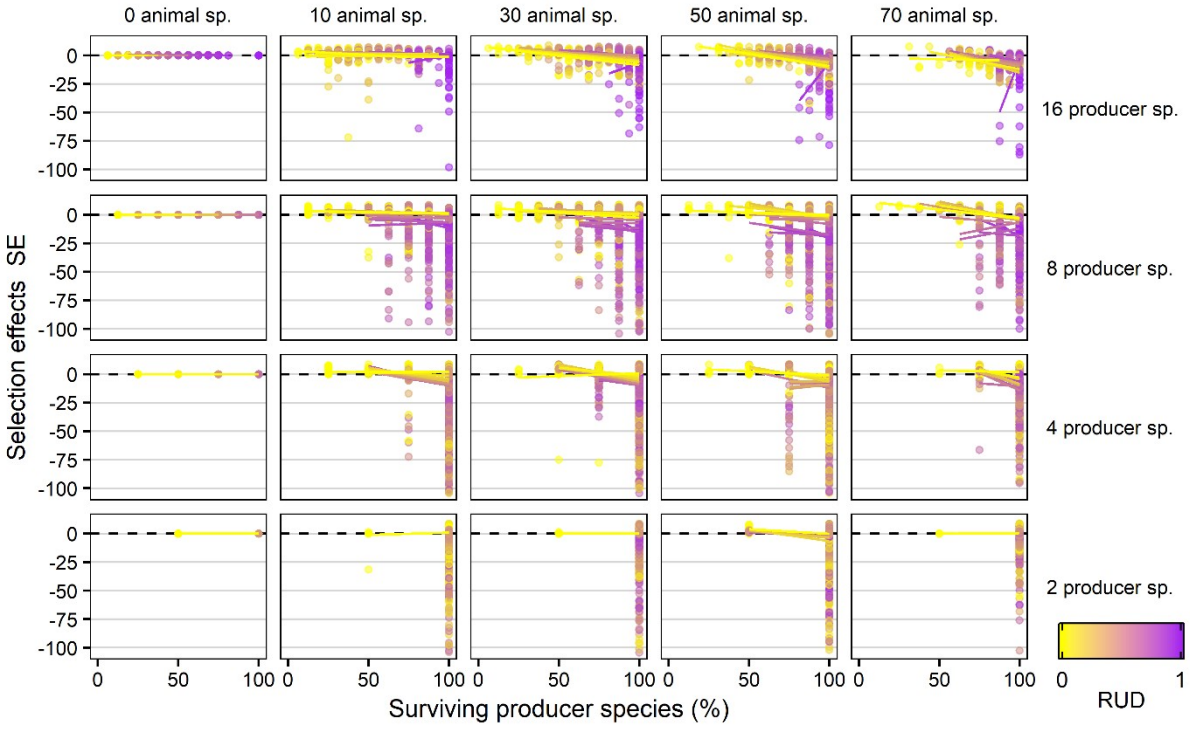

Figure S9: Effects of relative primary producer species survival on net diversity effects ΔY. Effects are shown for different levels of producer (rows) and multi-trophic animal richness (columns). The level of resource-use dissimilarity (RUD) is indicated by the color (yellow: low, purple: high). To improve readability, only 95% of the simulated food webs are shown.

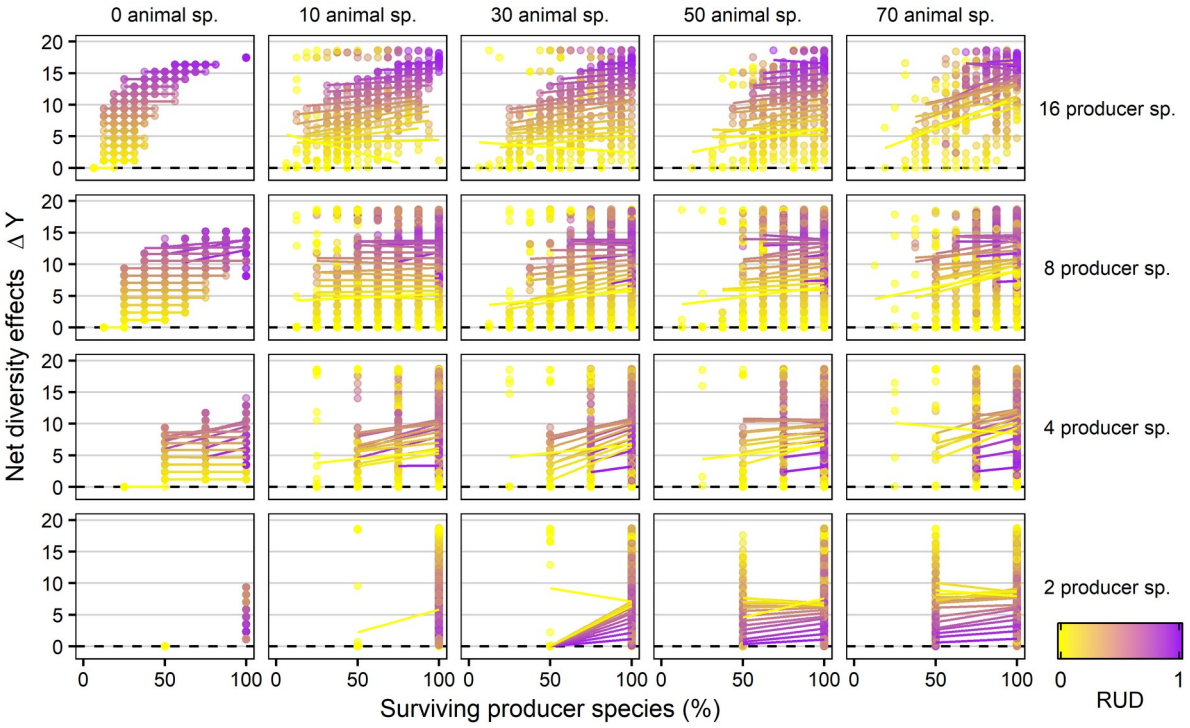

Figure S10: Effects of relative primary producer species survival on the $\log_{10}$ biomass of the surviving producer species. Effects are shown for different levels of producer (rows) and multi-trophic animal richness (columns). The level of resource-use dissimilarity (RUD) is indicated by the color (yellow: low, purple: high).

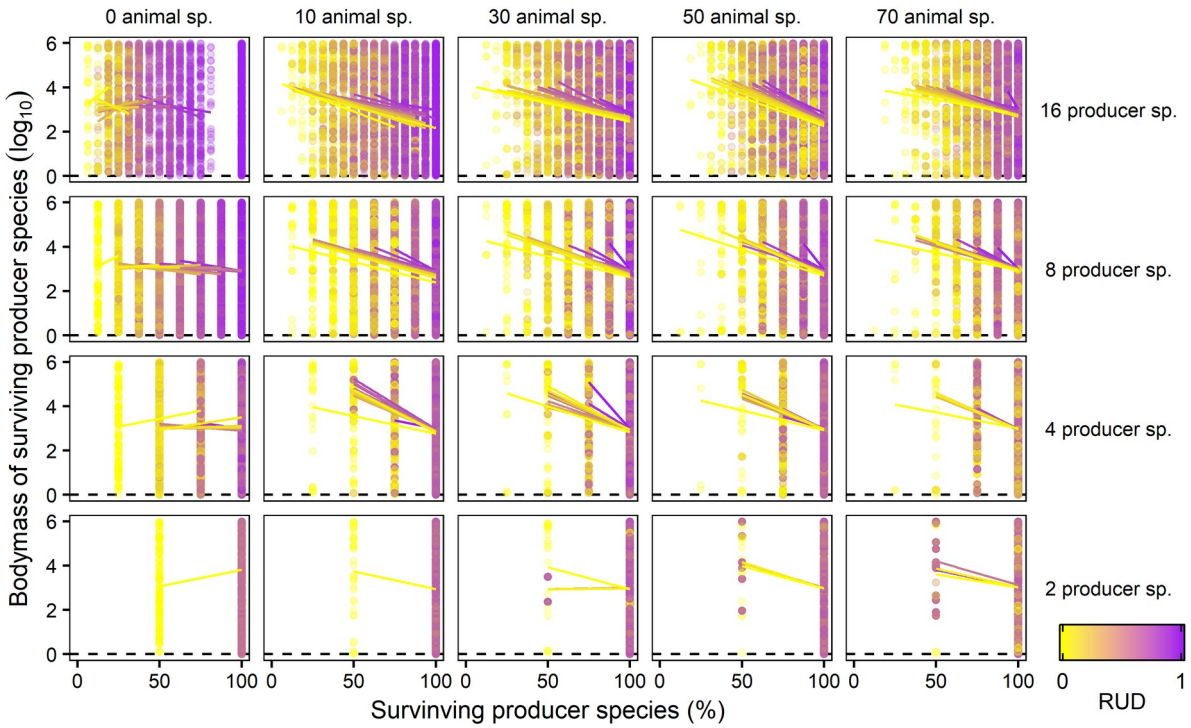

Figure S11: Effects of $\log_{10}$ biomass of the surviving producer species on their productivity relative to their maximum possible productivity (i.e., used resources / accessible resource). Effects are shown for different levels of producer (rows) and multi-trophic animal richness (columns). The level of resource-use dissimilarity (RUD) is indicated by the color (yellow: low, purple: high).

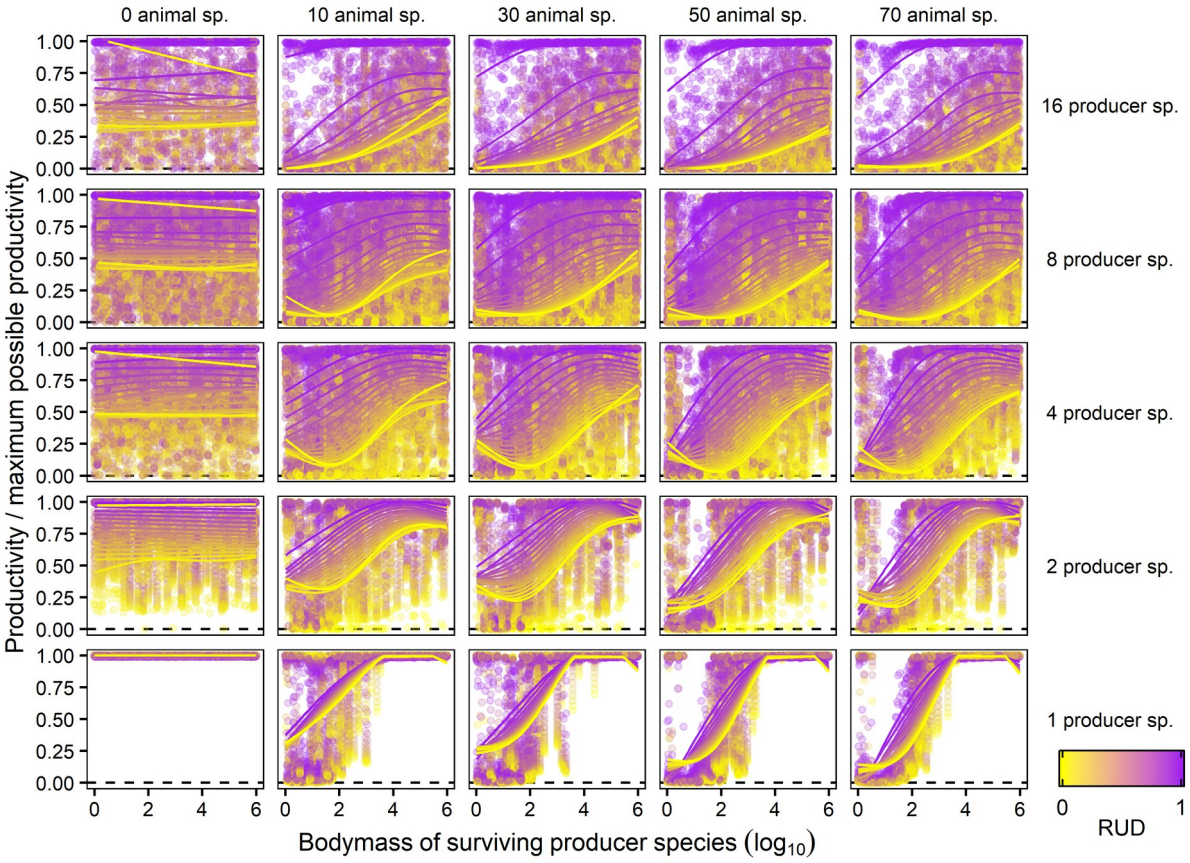

Figure S12: Effects of resource-use dissimilarity RUD on the relative survival of the animal community. Effects are shown for different levels of producer (rows) and multi-trophic animal richness (columns). Error bars show 25th and 75th; squares show 50th percentile (i.e., median).